PII: S0955-2219(97)00021-6

Pressureless Sintering of Al_2O_3/SiC_W Materials: Effect of the Reducing Atmosphere

G. Urretavizcaya, J. M. Porto López & A. L. Cavalieri

Instituto de Investigaciones en Ciencia y Tecnología de Materiale (INTEMA)-(UNMdP-CONICET)
Juan B. Justo 4302 (7600) Mar del Plata, Argentina

Abstract

The effect of the temperature and the conditions of the reducing atmosphere on the sintering behavior of pressureless-sintered Al_2O_3/SiC_W composites was studied by SEM, XRD and density measurements and analyzed throughout a thermodynamic study of the system. Different partial pressures of oxygen were estimated for two ways of arrangement of the samples, between graphite disks or packed in an SiC bed, the former being lower. A higher amount of glassy phase was observed when pressureless sintering was conducted with samples between graphite disks and at the highest sintering temperature studied (1800°C). Taking into account the reactions that can occur at the partial oxygen pressures thermodynamically estimated, the formation of a high amount of liquid was explained throughout two mechanisms: formation of a melt with the composition of the eutectic of the Al_2O_3–Al_4C_3 binary system and liquid production by reaction of SiC and Al_2OC. The higher densities reached at 1800°C than at 1700°C were attributed to a liquid-phase assisted mechanism of sintering. © 1997 Elsevier Science Limited.

1 Introduction

SiC whisker-reinforced Al_2O_3 composites (Al_2O_3/SiC_W) have been extensively studied in recent years because of their improved mechanical properties.[1-10] Due to the presence of whiskers, which makes densification difficult, great effort was dedicated to the study of hot pressing, in order to obtain high densities.[3-5] However, this process of sintering presents several limitations in size and geometry of the samples, together with a high cost.[11,12]

Other sintering routes have been studied resulting in a possible alternative: the pressureless sintering, in an atmosphere with low oxygen partial pressure in order to avoid SiC oxidation, and optimizing raw materials, processing steps and sintering conditions.

Barclay *et al.*[13] studied the sintering of Al_2O_3/SiC_W composites in a graphite furnace in Ar at 1500 and 1800°C, using graphite crucibles. They observed a significant inhibition of densification caused by the whiskers resulting in densities as low as 63% in SiC_W(13 vol%)/Al_2O_3 composites. However, an improvement in densification was achieved through the incorporation of yttrium oxide. Kim and Lee[14] studied the densification of materials with 15 vol% of SiC whiskers by hot pressing and pressureless-sintering, achieving relative densities of 98 and 95%, respectively. Densification of Al_2O_3 reinforced with SiC platelets sintered in an SiC bed under Ar at 1700°C was studied by Belmonte *et al.*,[15] obtaining a relative density of 96% when the SiC content was 5 vol%. These authors reached the same relative density for 12 vol% of SiC using gas pressure sintering.[15]

On the other hand, it has been reported that, in conditions of high temperature and low oxygen partial pressure, several reactions like aluminium oxide decomposition, formation of carbides and oxycarbides and formation of liquid phase can be produced.[16-24] Al_2OC can be formed by reaction between carbon monoxide and gaseous aluminium.[19] Moreover, a permanent melt with the composition of the eutectic in the Al_2O_3–Al_4C_3 system[20,21] or a silicate glass due to the reaction between Al_2O_3, Al_4C_3 and SiC[22] can be produced.

The analysis of the results given above leads to the affirmation that a control of the sintering atmosphere is essential in this kind of system. The

objective of this work is the study of the pressure-less sintering of Al_2O_3/SiC_W composites in different conditions of atmosphere and temperature, and the interpretation of the observed results throughout a thermodynamic analysis of the system.

2 Experimental

Samples with 0, 5, 10 and 15 vol% of SiC whiskers were prepared from Al_2O_3 powder (Reynolds RC-HP DBM, average particle size $0.35\,\mu m$) and SiC whiskers (Tateho SCW-1, $35\,\mu m$ in length and $0.5\,\mu m$ in diameter) added as the reinforcing phase. Chemical analyses of both Al_2O_3 and whiskers are given in Table 1.

Green samples of both Al_2O_3 and Al_2O_3/SiC_W composite materials were prepared by slip casting of aqueous suspensions of Al_2O_3 powders and SiC whiskers, drying the compacts at room temperature and precalcining at 950°C for 90 min before sintering. In order to improve the green densities of the compacts, some of the samples were impregnated with $Al(NO_3)_3$ following a procedure described in a previous work.[25]

Samples were pressureless-sintered in a graphite-element resistance furnace (ASTRO Group 1000), in He atmosphere during 220 min. Two series of experiments were conducted: samples pressureless-sintered at 1800°C packed in an SiC bed or arranged between graphite disks, and impregnated samples pressureless-sintered at 1700 and 1800°C, between graphite disks.

XRD analyses (Philips) were made using Ni-filtered Cu K_α radiation.

The densities were determined by the Archimedes method in water and the relative density values were calculated using the theoretical densities of α-Al_2O_3 ($3.98\,g\,cm^{-3}$), SiC ($3.20\,g\,cm^{-3}$) and γ-Al_2O_3 ($3.50\,g\,cm^{-3}$).

Table 1. Chemical analyses (wt%) of Al_2O_3 powder and SiC whiskers

Compound	Al_2O_3	SiC_W
SiO_2	0·170	0·100
Fe_2O_3	0·020	0·080
TiO_2	0·001	0·008
CaO	0·020	0·200
MgO	0·047	0·030
Na_2O	0·060	0·008
K_2O	0·017	0·004
Al_2O_3	99·235*	0·230
SiC	—	99·340*
W.L. (1000°C)	0·430	—

*Values calculated by difference.

A quantitative determination of the amount of silicate glass in the sintered specimens was made by leaching. Powdered samples were treated with 20% HF (1 g powder $10\,ml^{-1}$ HF) at room temperature during 15 min, with agitation. Powders were filtered, washed and dried. After firing at 900°C for 1 h, the weight losses were measured.

The microstructure of the samples was examined on fracture surfaces by scanning electron microscopy (Philips 505).

3 Results

3.1 Effect of the arrangement of the samples

Figure 1 shows the microstructures of the samples containing the lowest and the highest SiC_W amounts pressureless-sintered at 1800°C arranged in an SiC bed (a and c) or between graphite disks (b and d).

In both series of samples, a glassy phase can be observed. However, the amount of the glassy phase is higher in the samples sintered between graphite disks. This is in agreement with the results of the quantitative analysis of the glass (1·5% in SiC bed and 3·2% in graphite disks for 15 vol% of SiC) performed by HF leaching.

A progressive increment in the amount of liquid with the increment in SiC_W content was also observed (Fig. 1) for each series. Thus, in SiC_W (15 vol%)/Al_2O_3 samples sintered between graphite disks, Al_2O_3 grains cannot be clearly distinguished, and just a little amount of SiC_W is observed. A chemical etching with boiling H_3PO_4, which dissolves the melt and the Al_2O_3 matrix, revealed the SiC whiskers (Fig. 2).

Additionally, both series of samples (arranged in an SiC bed or between graphite disks) show a progressive diminution in Al_2O_3 grain size as the SiC_W content increases (Fig. 1).

An XRD study was made on the surface of the samples in order to analyze the area of the materials directly exposed to the atmosphere. In all the samples sintered between graphite disks, Al_2OC was observed, and those containing whiskers also showed Al_4SiC_4 phase.

Final apparent and relative densities of Al_2O_3 and SiC_W/Al_2O_3 composites without impregnation, pressureless-sintered at 1800°C in SiC bed and between graphite disks, are given in Table 2. It can be observed that density values diminish with the increment in whiskers content in both series. On the other hand, for all the SiC_W contents used, densities achieved on samples pressureless-sintered
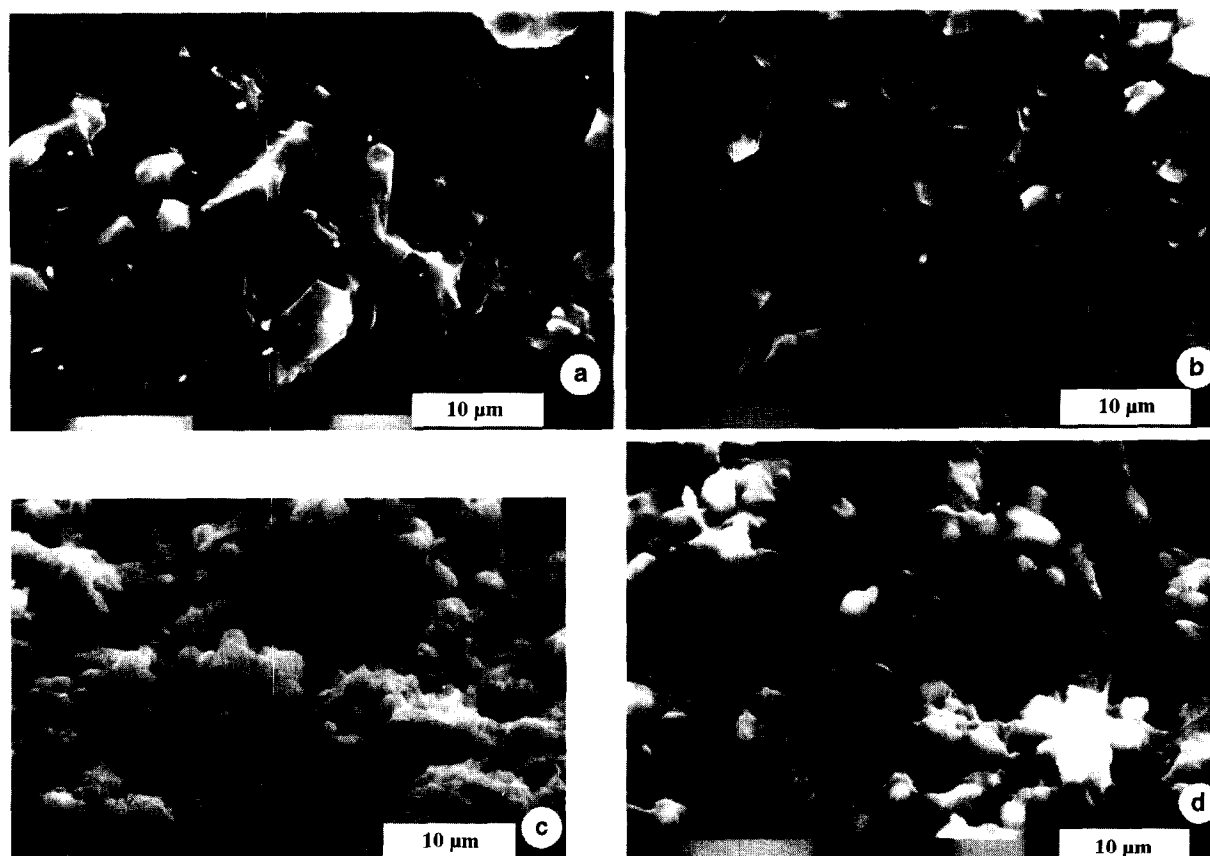
Fig. 1. SEM micrographs of SiC_W(5 and 15 vol%)/Al_2O_3 samples pressureless-sintered at 1800°C in SiC bed (a and c) and between graphite disks (b and d).

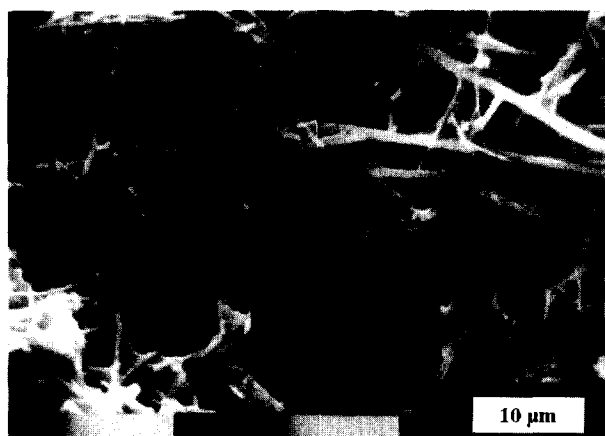**Fig. 2.** SEM micrograph of SiC_W(15 vol%)/Al_2O_3 sample pressureless-sintered at 1800°C between graphite disks etched with boiling H_3PO_4.

between graphite disks were higher than those obtained using SiC bed.

Table 3 shows the weight losses measured after sintering. These weight losses increase with the increment of whiskers content, and higher values for samples sintered between graphite disks were registered.

3.2 Effect of the temperature

This part of the study was made on impregnated samples arranged between graphite disks. In these conditions, an improvement in densification is achieved resulting in microstructures with lower porosity and homogeneous grain size.[25]

Figures 3(a) and 3(b) show the SEM micrographs of the microstructure of 15 vol% SiC_W/Al_2O_3 composite pressureless-sintered between graphite disks at 1700 and 1800°C, respectively. Differences in the amount of liquid phase present in the two samples are observed. At 1800°C, there was a more extensive formation of liquid than at 1700°C, in agreement with the results of the quantitative analysis of glass in which the same trend was determined (3·2 and 1·6% at 1800 and 1700°C, respectively).

Although the Al_2O_3 grain size was smaller in samples treated at 1700°C than in those sintered at 1800°C (Figs 4(a) and 4(b)), the microstructure that resulted was more homogeneous at the higher temperature. Samples sintered at 1700°C show a bimodal distribution of grains with sizes of 10 and 2–3 μm, while those sintered at 1800°C exhibit a very uniform grain size (15 μm). The last samples show a microstructure characteristic of a liquid

Table 2. Apparent and relative densities of non-impregnated alumina samples with different contents of whiskers, pressureless-sintered at 1800°C in an SiC bed or between graphite disks

SiC_W content (vol%)	Arrangement of the samples			
	SiC bed		Graphite disks	
	Apparent density (g cm^{-3})	Relative density (%)	Apparent density (g cm^{-3})	Relative density (%)
0	3·50	88	3·70	93
5	2·84	72	3·36	85
10	2·67	68	3·10	79
15	2·48	64	2·72	70

phase-assisted sintering[29,32,33] with faceted grains and tabular alumina, which supports the above analysis.

Table 4 shows apparent and relative densities for impregnated samples sintered at 1700 and 1800°C between graphite disks.

At the sintering temperatures studied, a decrease in the densification of the samples with the increment of SiC_W content was observed. The density values measured after sintering at 1800°C are slightly higher than those obtained at 1700°C.

At 1800°C, the density values of impregnated samples (Table 4) are higher than that of the non-impregnated ones (Table 2).

4 Thermodynamic analysis of the system

In order to better understand the complex system under study, a thermodynamic analysis of the atmosphere and the reactions that could take place in the present sintering conditions has been done.

4.1 Oxygen partial pressure

The equivalent oxygen partial pressures have been estimated from the curves of oxygen pressure as a function of both the CO_2/CO pressure ratio and the temperature (Fig. 5). In order to draw these curves, the JANAF thermochemical tables data[26] were used. The pressures of the present species were determined by the following equilibrium reactions:

$$2\,CO_{(g)} \Longleftrightarrow C_{(graphite)} + CO_{2(g)} \qquad (1)$$

$$2\,CO_{2(g)} \Longleftrightarrow 2\,CO_{(g)} + O_{2(g)} \qquad (2)$$
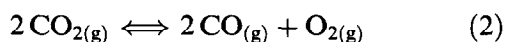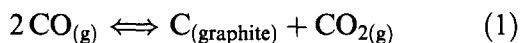
According to the phase rule, this system, with two components (carbon and oxygen) and two phases, has two degrees of freedom. The bold curve in

Fig. 5 represents the divariant equilibrium situation, showing the CO_2/CO pressures ratios of the gaseous phase in equilibrium with graphite as a function of the temperature at a total pressure of 1 atm.

When samples are arranged between graphite disks, the system is graphically situated on the left of the bold curve in Fig. 5 (shaded area represents metastable conditions with excess of precipitated graphite). The oxygen partial pressures are lower than those corresponding to the equilibrium with precipitated graphite at each temperature (about $3 \cdot 10^{-15}$ atm at 1800°C and $1 \cdot 10^{-15}$ atm at 1700°C).

On the other hand, when an SiC bed is used to pack the samples, the conditions of the sintering atmosphere are those of a system without precipitated graphite. Thus, the situation is represented in Fig. 5 on the right of the bold curve (unshaded area represents conditions under which a gaseous phase is in stable equilibrium without precipitation of carbon). The system has now an additional degree of freedom because the number of phases has decreased by one with respect to the situation previously analyzed.[27] The oxygen partial pressure is at least higher than that corresponding to the equilibrium pressure.

According to the above analysis, an SiC powder bed, used to modify the sintering atmosphere leads to lesser reducing conditions than those corresponding to the system with excess of carbon (disks of graphite), in agreement with literature.[28]

Table 3. Weight losses of alumina samples with different contents of whiskers, after pressureless-sintering at 1800°C in a SiC bed or between graphite disks

SiC_W content (vol%)	Weight loss (%)	
	SiC bed	Graphite disks
0	—	4·6
5	0·4	5·3
10	0·9	6·4
15	1·6	7·3

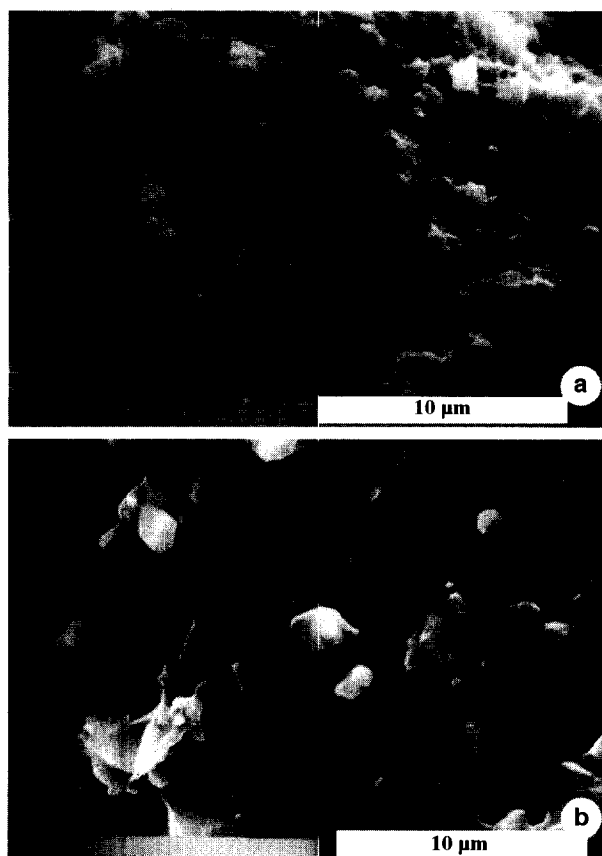**Fig. 3.** SEM micrographs of impregnated SiC$_W$(15 vol%)/Al$_2$O$_3$ samples pressureless-sintered between graphite disks at 1700°C (a) and 1800°C (b).
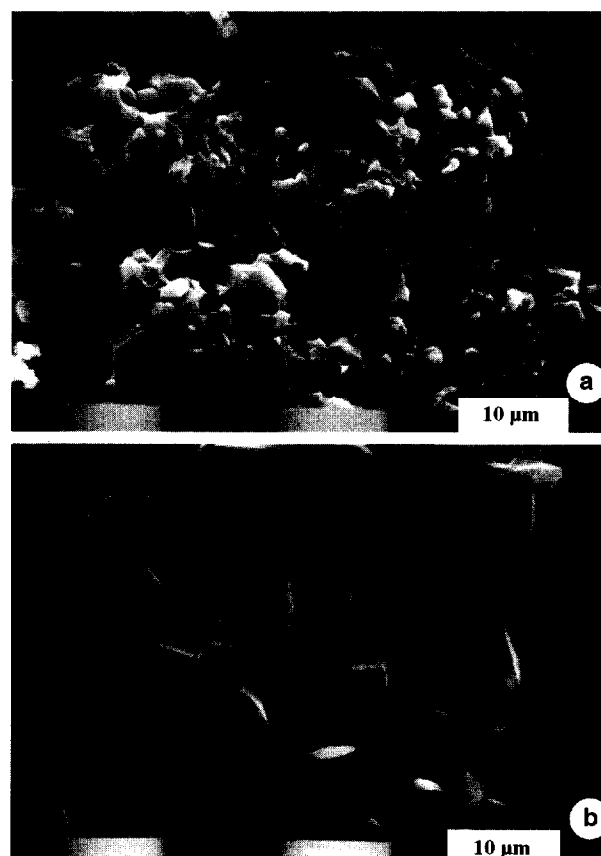

Fig. 4. SEM micrographs of impregnated Al$_2$O$_3$ samples pressureless-sintered between graphite disks at 1700°C (a) and 1800°C (b).

4.2 Decomposition of Al$_2$O$_3$

From the Ellingham diagram for the formation of oxides,[27] it was concluded that, at 1800°C, decomposition of Al$_2$O$_3$ can occur if the oxygen partial pressure is lower than 10^{-17} atm, according to the following reaction:

$$Al_2O_{3(s)} \Longleftrightarrow 2\,Al_{(l,g)} + 3/2\,O_{2(g)} \qquad (3)$$
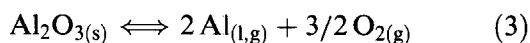
Taking into account the O$_2$ partial pressure values estimated in Section 4.1 for systems with SiC bed or graphite disks, Al$_2$O$_3$ decomposition could only be expected in the second condition.

4.3 Formation of Al$_4$C$_3$

Other reactions thermodynamically feasible in atmospheres with low oxygen pressure have been considered. In order to analyze the conditions for the formation of aluminum carbide from aluminum oxide, free energy variation vs temperature was calculated using data from JANAF tables[26] for the following reaction:

$$2/3\,Al_2O_{3(s)} + C_{(s)} \Longleftrightarrow 1/3\,Al_4C_{3(s)} + O_{2(g)} \qquad (4)$$
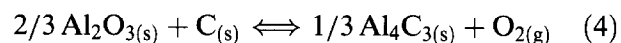
The obtained values (bold curve) and the curves that represent the equilibrium among CO, O$_2$ and

Table 4. Apparent and relative densities of impregnated alumina samples with different whisker contents, pressureless-sintered between graphite disks at 1700 and 1800°C

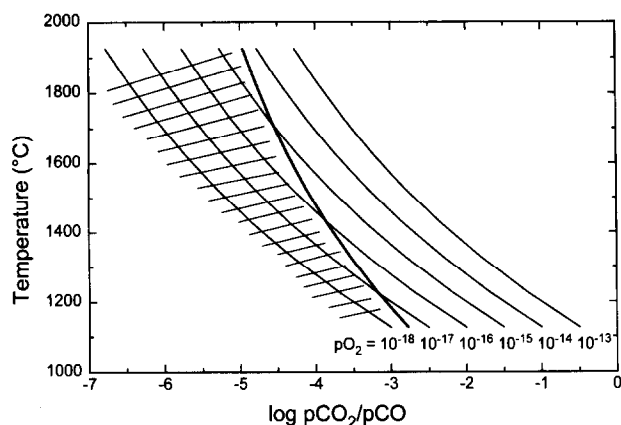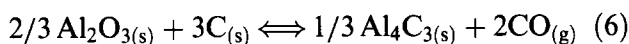| SiC$_W$ content (vol%)	Sintering temperature			
	1700°C		1800°C	
	Apparent density (g cm^{-3})	Relative density (%)	Apparent density (g cm^{-3})	Relative density (%)
0	3·69	93	3·86	97
5	3·39	86	3·43	87
10	3·15	80	3·24	83
15	3·07	79	3·07	79

Fig. 5. Curves of partial pressure of oxygen as a function of CO_2 and CO pressures ratio and temperature at a total pressure of 1 atm, based on data of JANAF tables.[26]

precipitated graphite calculated for three partial pressures of CO: 1, 0·1 and 0·01 atm (dashed curves) are shown in Fig. 6. The oxygen partial pressure in presence of excess of carbon is given by the following equilibrium:

$$2 CO_{(g)} \Longleftrightarrow 2 C_{(s)} + O_{2(g)} \qquad (5)$$
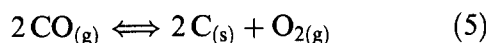
By substraction of eqn. 4 and eqn. 5:

$$2/3\, Al_2O_{3(s)} + 3C_{(s)} \Longleftrightarrow 1/3\, Al_4C_{3(s)} + 2CO_{(g)} \qquad (6)$$

The intersections of the solid curve and the dashed ones represent the lower temperature at which aluminum carbide can be formed by reaction (6) at each CO pressure. This temperature diminishes from 1993°C ($p_{CO} = 1$ atm) to 1775 and 1583°C ($p_{CO} = 0·1$ and 0·01 atm, respectively). In our sintering conditions, the CO partial pressure is at least lower than 0·33 atm (the value which corresponds to a closed system with precipitated graphite, in presence of air). This affirmation is supported by the results of a study performed in a similar system, in which a partial pressure of CO as low as 0·003 atm at 1800°C was determined.[19]

From the above analysis, it can be inferred that, at 1800°C, the formation of Al_4C_3 from Al_2O_3 is a feasible reaction. However, from Fig. 6 only if the CO partial pressure is lower than 0·1 atm, could Al_4C_3 be formed at 1700°C.

4.4 Formation of Al_2OC

In the sintering conditions of this work, Al_2OC can be formed. It can be affirmed taking into account the results of Lefort *et al.*[19] These authors determined the existence of a range of CO partial pressures in which the Al_2OC can be formed from CO
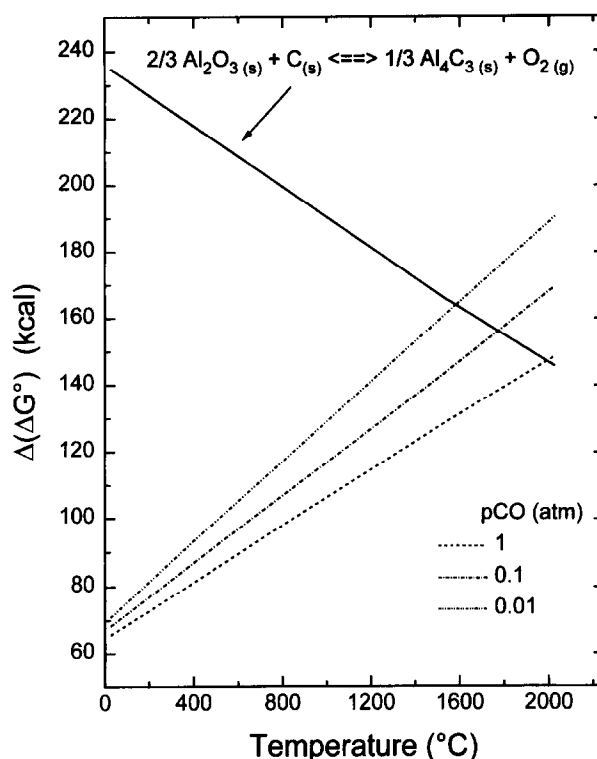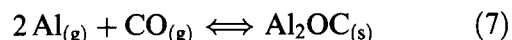

Fig. 6. Differences in free energy of formation between Al_4C_3 and Al_2O_3 as a function of the temperature. CO/O_2/graphite equilibria at three CO pressures (1, 0·1 and 0·01 atm) are also shown. (Based on data of JANAF tables).[26]

and gaseous aluminum produced by decomposition of Al_2O_3 according to the following reaction:

$$2\, Al_{(g)} + CO_{(g)} \Longleftrightarrow Al_2OC_{(s)} \qquad (7)$$

The Al–CO–Al_2OC equilibrium is shifted towards the decomposition of oxycarbide if the partial pressure of CO is lowered.[19]
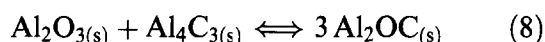
4.5 Formation of a melt

In our sintering conditions, the formation of a melt can be possible at low oxygen partial pressure and high temperature (1800°C). Two mechanisms proposed in the literature are considered adequate to explain the presence of a melt in these conditions: (a) the formation of a melt with the composition of the eutectic in the Al_2O_3–Al_4C_3 system,[20,21] and (b) a liquid produced simultaneously with the Al_4SiC_4 formation.[22]

(a) Larrère *et al.*[21] reviewed and modified the phase equilibrium diagram of the Al_2O_3–Al_4C_3 binary system, which was first established by Foster *et al.*[20] This system shows an eutectic point with the composition 90 mol% Al_2O_3–10 mol% Al_4C_3 whose melting temperature is slightly lower than 1815°C. Moreover, a meta-

stable phase-equilibrium diagram for this system, which lowers the eutectic melting point down to 1800°C was presented.[21]

From the above analysis, and taking in mind the possibility of Al_4C_3 formation at 1800°C when graphite disks are used (Section 4.3), it was concluded that a permanent melt with the composition of the eutectic point can be formed if this composition is locally reached. At 1700°C, the eutectic point temperature is not reached; so, even though there was Al_4C_3 formation, a permanent melt could not be produced in the system.

(b) The second possibility of melt formation is the mechanism proposed by Oscroft *et al.*:[22] aluminum silicon carbide and liquid are formed by the following reactions:

$$Al_2O_{3(s)} + Al_4C_{3(s)} \Longleftrightarrow 3\,Al_2OC_{(s)} \qquad (8)$$

$$Al_2OC_{(s)} + SiC_{(s)} \Longleftrightarrow Al_4SiC_{4(s)} + liquid \qquad (9)$$

Reaction (9) can be also produced with Al_2OC formed by reaction (7), Section 4.4. At 1700°C, this mechanism can operate if the samples contain SiC whiskers.

4.6 Weight losses

The partial dissociation of Al_2OC at high temperatures and the reaction of SiC and Al_2O_3 at low oxygen partial pressures giving gaseous products as follows

$$SiC_{(s)} + Al_2O_{3(s)} \Longleftrightarrow SiO_{(g)} + CO_{(g)} + Al_2O_{(g)} \qquad (10)$$
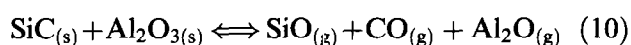
are responsible for the weight losses produced during sintering, as proposed by Oscroft *et al.*[22]

The last possibility is supported by the study performed by Misra,[17] who concluded that the predominant gaseous species in the SiC–Al_2O_3 system are SiO, CO, Al_2O and Al. This author also determined that 0·25 is the lowest carbon activity required for Al_4C_3 formation at 1800°C. In the present work, when the sintering conditions were samples arranged between graphite disks inside a graphite furnace, a carbon activity equal to unity can be assumed, supporting from another point of view the feasibility of Al_4C_3 formation.

5 Discussion

The obtained results, including developed microstructures and measured densities, are discussed in

this section taking into account the previous thermodynamic analysis.

In both series of samples, pressureless-sintered at 1800°C arranged in an SiC bed or between graphite disks, the observed glassy phase was expected because of the content of impurities of the alumina powder used in this work (0·335 wt%). It has been reported that a silicate glass is observed in sintered Al_2O_3 with a content of impurities of 0·25 wt%.[29]

However, the higher amount of this phase present in the samples sintered between graphite disks can only be explained by the presence of another kind of melt. It is proposed that this melt can be originated by the reactions described above that take place in the highest reducing atmosphere when graphite disks are used. At 1800°C, when conditions of very low O_2 partial pressure and low CO partial pressure prevail, the formation of Al_4C_3 from Al_2O_3 is a possible reaction (Section 4.3). Then, local Al_2O_3–Al_4C_3 equilibria could be reached with appearance of a melt at the eutectic temperature.[21] Furthermore, the contribution is proposed of a liquid phase produced by reaction of Al_2OC and SiC,[22] as discussed in Section 4.5(b).

The presence of Al_2OC and Al_4SiC_4 detected by XRD and the existence of Al_4C_3 justified by the thermodynamic study (reaction (6)) support that two mechanisms of melt formation take place. Al_4C_3, an intermediate in the formation of the permanent melt, was not detected by XRD analysis because it was totally consumed or due to its great instability in a wet atmosphere.

The presence of a higher amount of liquid when the SiC_W content increases is also explained throughout the mechanism proposed by Oscroft[22] (reactions (8) and (9)). According to reaction (9) SiC is a reagent in the liquid formation. The whiskers observed after etching with boiling H_3PO_4 confirm the presence of a melt and indicate that, although they are involved in melt formation, they are not totally consumed in the reaction.

The decrease in the densities of Al_2O_3 and SiC_W/Al_2O_3 composites without impregnation, pressureless-sintered at 1800°C in SiC bed and between graphite disks, reflects the same trend observed in green densities, where the presence of the whiskers difficults the compaction of the samples.[30] However, the diminution of the values of 10 and 15 vol% SiC_W/Al_2O_3 composites is higher than that expected only from the differences in their green densities. This fact is associated to an additional inhibiting effect of the whiskers which interfere with shrinkage in sintering by crosslinking among themselves.[30,31]

The higher densities achieved on samples pressureless-sintered between graphite disks than those obtained using SiC bed is a consequence of the higher amount of melt present in the samples sintered between graphite disks, which favors a mechanism of liquid phase sintering resulting in an improvement of densification.

Additionally, the weight losses, higher as the whiskers content increases and also in samples pressureless-sintered between graphite disks, were attributed to the possibility of Al_2O_3 and Al_2OC decompositions (reactions (3) and inverse (7)) and to the reaction between Al_2O_3 and SiC to form gaseous products (reaction (10)).

Comparing the microstructures obtained at 1700 and 1800°C, the liquid observed can be originated by the impurities present on the starting materials and another liquid arising by reaction of Al_2OC and SiC (reaction (9)) at both temperatures. At 1800°C, the greater amount of liquid observed can be attributed to the simultaneous formation of a permanent melt in the Al_2O_3–Al_4C_3 binary system. However, at 1700°C, this kind of melt is not expected to be produced because of the temperature is lower than that of the invariant point,[21] despite the possible Al_4C_3 formation (Section 4.3).

The higher densities obtained at the higher temperature studied (1800°C) were attributed to a liquid phase-assisted sintering mechanism. However, the increase is slight, probably due to an opposite effect of weight loss only produced in the more extremely reducing atmosphere at 1800°C.

The improvement in the densification of the impregnated samples sintered at 1800°C is a consequence of both its higher precalcined densities and the greater reactivity of the small particles incorporated during impregnation.[25]

6 Conclusions

The oxygen partial pressures at 1800 and 1700°C in equilibrium with precipitated graphite at a total pressure of 1 atm were estimated (about $3 \cdot 10^{-15}$ atm and $1 \cdot 10^{-15}$ atm, respectively). The SiC used to pack the samples leads to lesser reducing conditions than those corresponding to the system with excess of graphite (samples arranged between graphite disks). The oxygen pressures are at least higher than the equilibrium values in the first situation and lower in the second condition.

At 1800°C, a higher amount of glassy phase was formed in samples sintered between graphite disks than in samples sintered in an SiC bed. In this last situation, the melt is attributed only to the presence of impurities in the Al_2O_3 powder. In the first condition, the melt is due to the impurities, but also to its formation by two mechanisms that can operate in the used sintering atmosphere: (a) formation of a melt with the composition of the eutectic of the Al_2O_3–Al_4C_3 binary system, because it is possible the formation of Al_4C_3 from Al_2O_3 and local equilibria could be reached, and (b) formation of a liquid together with Al_4SiC_4 by reaction of SiC and Al_2OC. The oxycarbide can be formed by reaction between CO and gaseous aluminium produced by decomposition of Al_2O_3 or by reaction between Al_2O_3 and Al_4C_3. The presence of a higher amount of liquid when the SiC_w content increases is also explained throughout mechanism (b).

At low oxygen partial pressures estimated at 1800°C with samples sintered between graphite disks, it was established that it is possible the Al_2O_3 and Al_2OC decomposition and the reaction of Al_2O_3 and SiC give gaseous products. An associated loss of material in detriment of final densities was determined.

At 1700°C and samples between graphite disks, the little amount of melt was attributed to impurities and to a minor contribution of liquid arising by reaction between Al_2OC and SiC. Permanent melt with the eutectic composition cannot be produced at this temperature.

At both temperatures, the progressive diminution in Al_2O_3 grain size and the decrease in the densification observed as the SiC_w content increases were attributed to the inhibiting effect of the whiskers on sintering. On the other hand, although the Al_2O_3 grain size was smaller in samples treated at 1700°C than at 1800°C, the microstructure that resulted was more homogeneous at the higher temperature. A bimodal grain size distribution was obtained at 1700°C, while at 1800°C very uniform grain size was observed. A microstructure characteristic of liquid-phase sintering with faceted grains and tabular alumina was developed at 1800°C in samples arranged between graphite disks.

Higher densities were achieved at 1800°C for samples sintered between graphite disks than those of samples sintered in an SiC bed. Moreover, the values were lower when the temperature decreased (1700°C). The higher values were attributed to a liquid-phase assisted mechanism of sintering. Additionally, an increase in the density values in the impregnated samples was determined. This is due to the higher green densities of the samples and the greater reactivity of the small particles incorporated during impregnation.

Acknowledgement

References

1. Becher, P. F. and Tiegs, T. N., Whisker-reinforced ceramics. In *Engineered Materials Handbook Vol. 1, Composites*. ASM International, 1988, pp. 941–944.

2. Becher, P. F., Hsueh, C. H., Angelini, P. and Tiegs, T. N., Toughening behavior in whisker-reinforced ceramic matrix composites. *Journal of Am. Ceram. Soc.*, 1988, **71**, 1050–1061.

3. Govila, R. K., Fracture of hot-pressed alumina and SiC-whisker-reinforced alumina composite. *Journal of Mater. Sci.*, 1988, **23**, 3782–3791.

4. Smith, S. M., Singh, J. P. and Scattergood, R. O., Processing characterization of SiC-whisker-reinforced alumina-matrix composites. *Journal of Am. Ceram. Soc.*, 1993, **76**, 497–502.

5. Homeny, J., Vaughn, W. L. and Ferber, M. K., Processing and mechanical properties of SiC-whisker-Al₂O₃-matrix composites. *Am. Ceram. Soc. Bull.*, 1987, **66**, 333–338.

6. Buljan, S. T., Pasto, A. E. and Kim, H. J., Ceramic whisker- and particulate-composites: Properties, reliability, and applications. *Am. Ceram. Soc. Bull.*, 1989, **68**, 387–397.

7. Becher, P. F., Microstructural design of toughened ceramics. *Journal of Am. Ceram. Soc.*, 1991, **74**, 255–269.

8. Chokshi, A. H. and Porter, J. R., Creep deformation of an alumina matrix composite reinforced with silicon carbide whiskers. *Journal of Am. Ceram. Soc.*, 1985, **68**, C144–145.

9. Grewe, H., Dreyer, K. and Kolaska, J., Whisker-reinforced ceramics. *Ber. DKG*, 1987, **8/9**, 303–308.

10. Homeny, J., Vaughn, W. L. and Ferber, M. K., Silicon carbide whisker/alumina matrix composites: Effect of whisker surface treatment on fracture toughness. *Journal of Am. Ceram. Soc.*, 1990, **73**, 394–402.

11. Ezis, A. and Rubin, J. A., Hot pressing. In *Eng. Mat. Handbook Vol. 4, Ceramics and Glasses*. ASM International, 1991, pp. 186–193

12. Tuffe, S., Dubois, J., Jorand, Y., Fantozzi, G. and Barbier, G., Processing and fracture behaviour of hot pressed silicon carbide whisker reinforced alumina. *Ceram. Int.*, 1994, **20**, 425–432.

13. Barclay, S. J., Fox, J. R. and Bowen, H. K., Processing of pressureless-sintered SiC whisker-reinforced Al₂O₃ composites. *Journal of Mater. Sci.*, 1987, **22**, 4403–4406.

14. Kim, Y. W. and Lee, J. G., Pressureless sintering of Al₂O₃-SiC whisker composites. *Journal of Mater. Sci.*, 1991, **26**, 1316–1320.

15. Belmonte, M., Moya, J. S. and Miranzo, P., Obtención de materiales compuestos de Al₂O₃/plaquetas de SiC: efecto de las condiciones de procesado. *Bol. Soc. Esp. Cerám. Vidr.*, 1993, **32**, 133–139.

16. Nieto, M. I., Miranzo, P., de Aza, S. and Moya, J. S., Effect of the atmosphere on microstructural evolution of pressureless sintered Al₂O₃/SiC composites. *Journal of Ceram. Soc. Japan*, 1992, **100**, 459–462.

17. Misra, A. K., Thermochemical analysis of the silicon carbide-alumina reaction with reference to liquid phase sintering of silicon carbide. *Journal of Am. Ceram. Soc.*, 1991, **74**, 345–351.

18. Gadalla, A., Elmasry, M. and Kongachuichay, P., High temperature reactions within SiC-Al₂O₃ composites. *Journal of Mater. Res.*, 1992, **7**, 2585–2592.

19. Lefort, P., Tetard, D. and Tristant, P. Formation of aluminium carbide by carbothermal reduction of alumina: role of the gaseous aluminium phase. *Journal of Eur. Ceram. Soc.*, 1993, **12**, 123–129.

20. Foster, L. M., Long, G. and Hunter, M. S., Reactions between aluminum oxide and carbon. The Al₂O₃-Al₄C₃ phase diagram. *Journal of Am. Ceram. Soc.*, 1956, **39**, 1–11.

21. Larrère, Y., Willer, B., Lihrmann, J. M. and Daire, M., Diagrammes d'équilibre stable et métastable dans le système Al₂O₃-Al₄C₃. *Rev. Int. Hautes Tempér. Réfract. Fr.*, 1984, **21**, 3–18.

22. Oscroft, R. J. and Thompson, D. P., Influence of oxygen on the formation of aluminum silicon carbide. *Journal of Am. Ceram. Soc.*, 1992, **75**, 224–226.

23. Lihrmann, J. M., Zambetakis, T. and Daire, M., High-temperature behavior of the aluminum oxycarbide Al₂OC in the system Al₂O₃-Al₄C₃ and with additions of aluminum nitride. *Journal of Am. Ceram. Soc.*, 1989, **72**, 1704–1709.

24. Sata, T. and Sasamoto, T., Vaporization from Magnesia and Alumina Materials. In *Adv. in Ceramics, Vol. 10, Structure and properties of MgO and Al₂O₃ ceramics*, ed W. E. Kingery. Am. Ceram. Soc. Inc., Columbus, 1984, pp. 541–552.

25. Urretavizcaya, G., Cavalieri, A. L. and Porto López, J. M., Densification improvement of Al₂O₃-SiCw composites by impregnation. *Ceram. Int.*, 1995, **21**, 97–99.

26. JANAF Thermochemical Tables. *Journal of Phys. Chem. Ref. Data*, 1985, **14**(1).

27. Muan, A. and Osborn, E. F., *Phase Equilibria among Oxides in Steelmaking*. Addison-Wesley Publishing Company, Inc., Reading, MA, 1965.

28. Nieto, M. I., Miranzo, P., de Aza, S. and Moya, J. S., Effect of Atmosphere on Microstructural Evolution of Pressureless Sintered Al₂O₃/SiC Composites. *Journal of Ceram. Soc. Jap.*, 1992, **100**, 459–462.

29. Bateman, C. A., Bennison, S. J. and Harmer, M. P., Mechanism for the role of magnesia in the sintering of alumina containing small amounts of a liquid phase. *Journal of Am. Ceram. Soc.*, 1989, **72**, 1241–1244.

30. Sacks, M. D., Lee, H. W. and Rojas, O. E., Suspension processing of Al₂O₃/SiC whisker composites. *Journal of Am. Ceram. Soc.*, 1988, **71**, 370–379.

31. Tiegs, T. N. and Becher, P. F., Development of SiC-whisker-reinforced ceramics. *Am. Ceram. Soc. Bull.*, 1987, **66**, 339–342.

32. Hodge, J. D., The effect of particle size distribution on liquid phase sintering alumina. In *Ceram. Transactions, Vol. 7, Sintering of advanced ceramics*, ed. C. A. Handwerker, J. E. Blendell and W. A. Kaysser. Am. Ceram. Soc. Inc., Westerville, 1990, pp. 415–435.

33. Powell-Dogan, C. A., Heuer, A. H., Microstructure of 96% alumina ceramics: I Characterization of the as-sintered materials. *Journal of Am. Ceram. Soc.*, 1990, **73**, 3670–3676.